

PROCEEDINGS OF SPIE

[SPIDigitalLibrary.org/conference-proceedings-of-spie](https://spiedigitallibrary.org/conference-proceedings-of-spie)

Double drive modes unimorph deformable mirror with high actuator count for astronomical application

Ying Liu, Jianqiang Ma, Junjie Chen, Baoqing Li, Jiaru Chu

Ying Liu, Jianqiang Ma, Junjie Chen, Baoqing Li, Jiaru Chu, "Double drive modes unimorph deformable mirror with high actuator count for astronomical application," Proc. SPIE 9148, Adaptive Optics Systems IV, 91483Y (21 July 2014); doi: 10.1117/12.2055285

SPIE.

Event: SPIE Astronomical Telescopes + Instrumentation, 2014, Montréal, Quebec, Canada

Double Drive Modes Unimorph Deformable Mirror with high actuator count for astronomical application

Ying Liu¹, Jianqiang Ma², Junjie Chen¹, Baoqing Li^{1*}, Jiaru Chu¹

¹*Department of Precision Machinery and Precision Instrumentation, University of Science and Technology of China, Hefei, China*

²*Faculty of Mechanical Engineering & Mechanics, Ningbo University, Ningbo, China*

*Corresponding author: bqli@ustc.edu.cn

Unimorph deformable mirrors are attractive in adaptive optics system due to their advantages of simplicity, compact, low cost and large stroke. In this paper, a double drive modes unimorph deformable mirror is presented, which comprises a 200 μm thick PZT layer and a 400 μm thick silicon layer. This deformable has 214 inner actuators in the 50-mm active aperture, which are for the aberration correction and a outer ring actuator for generating an overall defocus bias. An analytical model based on the theory of plates and shells is built to predict the behavior of the deformable mirror. The stroke of the deformable mirror is tested in the experiments. In order to test the performance for aberration correction, the deformable mirror is used to correct the aberration from its imperfect initial mirror surface in the close-loop manner. The root-mean-square value of the mirror surface after the close-loop correction for ten iterations is about $\lambda/40$, which indicates this deformable mirror has a good aberration correction performance. This DM has the potential to be used for astronomical adaptive optics.

Key words: adaptive optics; unimorph deformable mirror; double drive mode; aberration correction performance.

1. Introduction

Adaptive optics (AO) was originally developed to compensate the turbulence-induced dynamic disturbance in astronomical telescope to improve the resolution [1,2]. Nowadays, nearly all modern large telescopes employ an AO system. The deformable mirror (DM), which works as the wavefront corrector, is the core component of the AO system. The traditional DM with thousands of piezoelectric stack actuator matches for astronomical AO. However, this device has a very high price [3].

Unimorph deformable mirrors are attractive in adaptive optics system due to their advantages of simplicity, compact, low cost and large stroke for correcting low-order optical aberrations (such as defocus, astigmatism, coma and spherical aberration) [4]. During past two decades, many kinds of unimorph DMs have been designed and fabricated [5-7]. Most of these DMs have no more than 100 actuators, and are designed for correction low-order aberrations.

In this paper, we develop a double drive modes unimorph DM with high actuator count for astronomical adaptive optics. This deformable mirror has 214 inner actuators in the 50-mm active aperture, which are for the aberration correction and a outer ring actuator for generating an overall defocus bias. The performance of this unimorph deformable mirror are presented.

2. Design of this unimorph DM

The layout of the double drive modes unimorph DM is illustrated in Fig. 1. The DM comprises of a 200 μm thick PZT layer and a 400 μm thick silicon layer. These two layers are glued together, with edge supported rigidly. The metallization on backside is patterned to produce 215 electrodes (one outer ring actuator, and 214 inner actuators which are arranged annularly). The uniform metallization between the silicon layer and the PZT layer is used as ground electrode. The overall size of the DM is 100 mm in diameter, with the effective diameter of 50 mm used for wavefront aberration correction. The diameter of the inner actuators' area is 60 mm, and the inner and outer diameter of the ring actuator is 64 mm and 90 mm, respectively. The inner actuator has a space of 4mm.

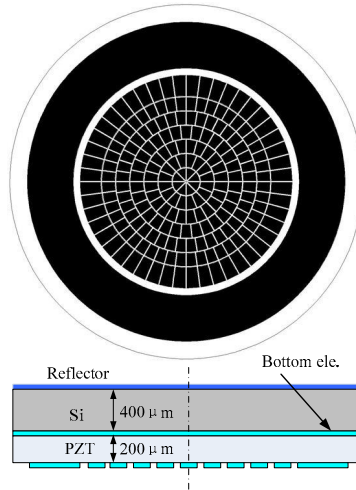


Fig. 1. Layout of unimorph DM: plan view of electrode pattern (top) and cross-sectional view of the unimorph DM (bottom).

In previous research[5], we have built the analytical model for simulating the behavior of the DM, which is based on the theory of plates and shells[8,9]. The schematic diagram of disk unimorph actuator is illustrated in Fig. 2. The actuator is divided into two sections: the central part covered by a circle electrode and the outer ring part. The deflection along the radius r and relative to point O_1 and point O_2 were represented by the following equations:

$$w_1(r) = \frac{M_0(b^2 - a^2)(a^2 - r^2)}{4D_e b^2} \quad (0 \leq r \leq a), \quad (1)$$

$$w_2(r) = \frac{M_0 a^2 [(r^2 - b^2) - 2b^2 \ln \frac{r}{b}]}{4D_e b^2} \quad (a \leq r \leq b), \quad (2)$$

where b and a are the radii of the DM and electrode, respectively. D_e is the equivalent flexural stiffness. M_0 is the moment caused by the PZT actuation:

$$M_0 = D_e \frac{-d_{31} U / h_{pzt}}{\frac{h}{2} + \frac{2}{h} \left(\frac{1}{E_{pzt} h_{pzt}} + \frac{1}{E_{si} h_{si}} \right) (D_{pzt} + D_{si})} \quad (3)$$

where U is the voltage applied on the PZT film and h is the total thickness of the actuator. D_{pzt} , E_{pzt} , h_{pzt} and d_{31} are the flexural stiffness, Young's modulus, thickness and transverse piezoelectric coefficient of the PZT film, respectively. D_{si} , E_{si} and h_{si} are the flexural stiffness, Young's modulus and thickness of the silicon elastic layer, respectively. Equations (1) to (3) can be also used to calculate the deformation of the outer ring actuator, by simply changing the deflection direction [5].

Based on this analytical model, we can predict the deformation of the inner actuators and the outer ring actuator. When all the inner actuators are driven by 50V and the outer ring actuator is driven by 55V, the two radial direction deformation curves are shown in Fig. 3. It can be found that when the deformable mirror is driven by positive voltage, the outer ring actuator and inner actuators generate deformation of two different directions. And these two deformations can be counteracted when appropriate voltages are applied on both the ring actuator and the inner actuators, resulting in a flat surface in the effective aperture of the deformable mirror, as shown in Fig. 3. So this double drive mode unimorph deformable mirror can generate deformations of two different directions driven by only positive voltages. To

correct aberrations, the ring electrode is normally biased at a constant voltage to produce a pre-deformed shape with an approximate deflection to the half of the maximum convex defocus generated by the inner actuators. The inner electrode voltages are varied to correct wavefront aberrations.

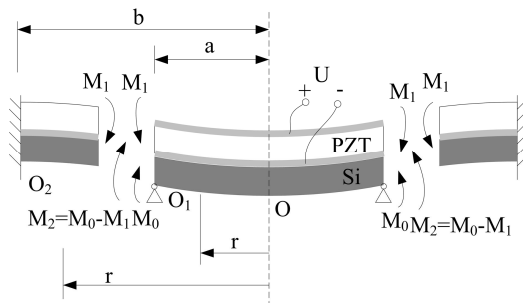


Fig. 2 Deflection of piezoelectric disk unimorph actuator. The actuator radius is b , the top electrode radius is a . M_0 : moment caused by actuation of PZT; M_1 : moment between two parts; M_2 : equivalent moment applied on the central part.

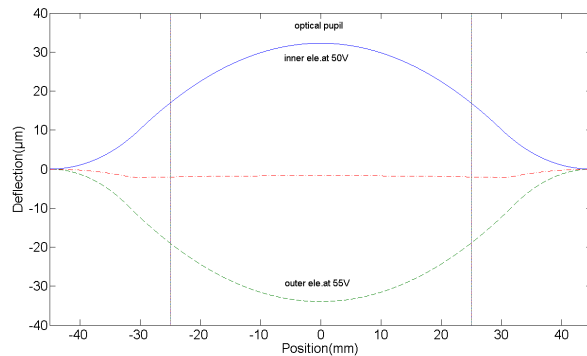


Fig. 3 The radial direction deformation curve of inner actuators and the outer ring actuator.

3. Experiment results

In the fabrication, a commercial available PZT film with silver electrode layers on both faces was used. The film has a diameter of 100 mm and a thickness of 200 μm . And a commercial 3-inches 400 μm thick silicon wafer is used as the structural layer. The inner electrodes and outer ring electrode are patterned with photoresist mask protection. The packaged DM is shown in Fig. 4. The package sizes are 200 mm, 160 mm, 60 mm, respectively. It can be found that this DM has the advantage of lightweight.



Fig. 4 The packaged double drive modes unimorph DM.

The performance of this DM was measured using Wyko RTI4100 with $\pm\lambda/20$ measurement accuracy ($\lambda = 0.633 \mu\text{m}$). Firstly, the deflection of the inner five rings of actuators were tested, where there are totally 118 actuators. The actuator deflections were measured by applying 50 V to a single actuator and performing a differential measurement (subtracting 0 V from test voltage measurement), and the measured actuator deflections are as shown in Fig. 5 and Tab. 1. It can be found that the actuator deflections are all about $1\mu\text{m}$ driven by 50V except the actuator on the first ring, which can meet the requirement of astronomy adaptive optics. The deflection of the outer ring actuator is also measured, as shown in Fig. 6. The deflection of the outer ring actuator is about $2.6633 \mu\text{m}$ when it is driven by 20V.

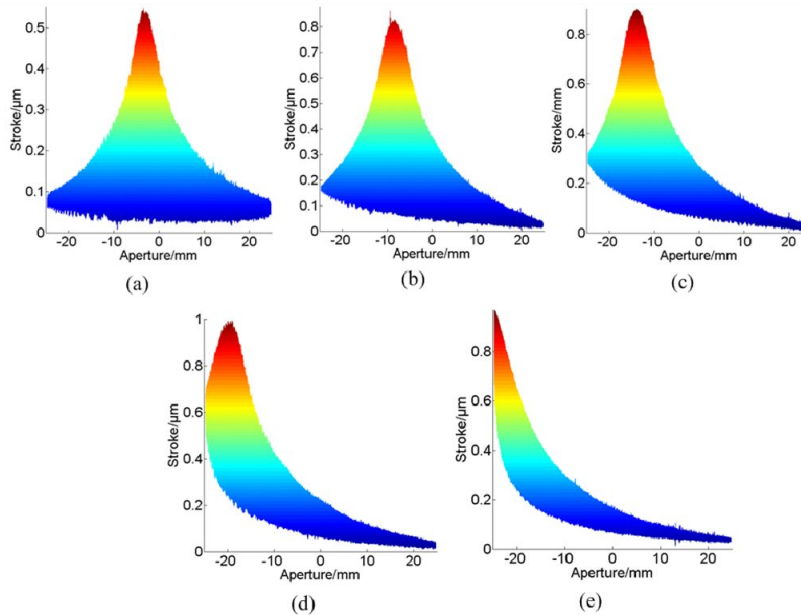


Fig. 5 Measured deflections of the inner actuator on different rings. (a)~(e) are the actuator deflection of the first ring to the fifth ring.

Tab. 1 Measured inner actuator deflections at 50V. Unit: μm

Ring	1	2	3	4	5
Deflection	0.5514	0.8787	0.9034	1.0005	0.9697

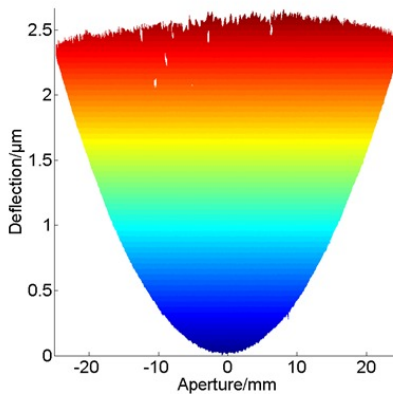


Fig. 6 Measured deflection of the outer ring actuator.

To test the aberration correction ability of this deformable mirror, the DM were used to correct the aberration from its initial surface. In aberration correction experiments, the inner 118 actuators were used to correct the aberrations in the aperture of 36 mm. The initial surface was also measured using Wyko RTI4100, as shown in Fig. 7. The PV value of the initial surface is $5.3207 \mu\text{m}$, and the rms value is $1.2088 \mu\text{m}$, with tip/tilt removed. From Fig. 7(b), it can be found that low order aberrations play a dominant role in the initial surface aberrations, which are relatively easy to be corrected.

The steepest descent algorithm was used to control the DM to correct the aberrations in the close-loop manner. The rms values of the residual aberrations are shown in Fig. 8. From the rms curve, it can be found that the rms value of the residual aberrations drops to 17.9 nm after ten iterations, with tip/tilt removed. The surface after correction is shown in Fig. 9. It can be found that the PV value of the surface after correction is 0.2608 μm , with tip/tilt removed. From the experiment results, it can be found that the rms value of the residual aberrations is close to $\lambda/40$, which indicates a good correction result has been achieved and this DM has a good aberration correction ability.

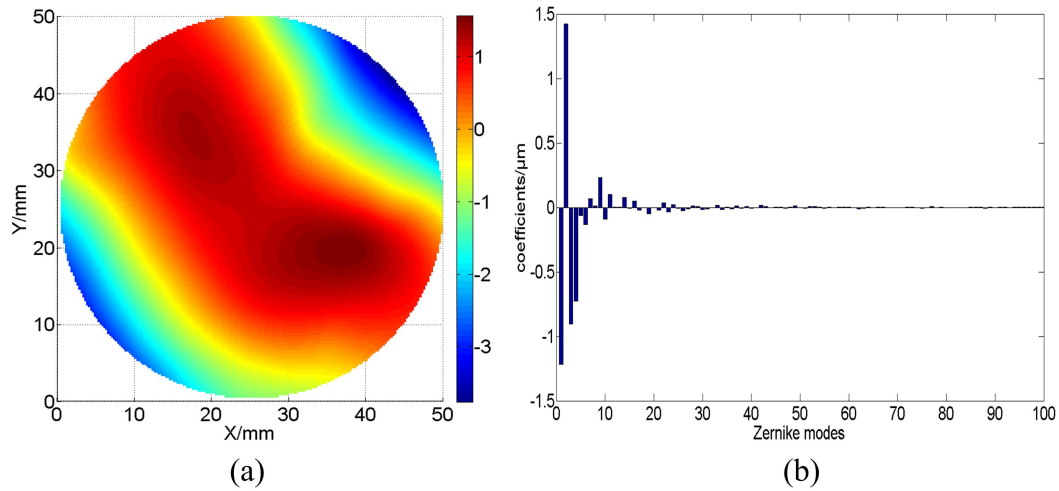


Fig. 7 Measured initial surface of the DM (a) and Zernike expansion coefficients of the initial surface.

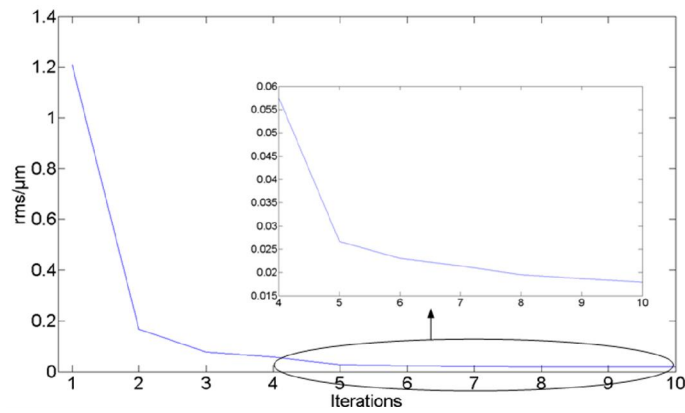


Fig. 8 The rms curve of the residual aberrations after correction.

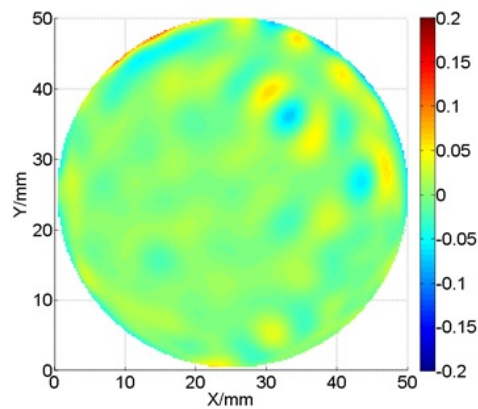


Fig. 9 Measured surface of the DM after aberration correction.

4. CONCLUSIONS

This paper reports a double drive modes unimorph deformable mirror with high actuator count for astronomical application. This unimorph deformable mirror can generate deformations of two different directions when it is driven by only positive voltages. The experimental actuator deflection is tested, which is about 1 μm at 50V. This deformable mirror is proved to have a have good aberration correction ability in the experiment of initial surface aberration correction. After correction, the rms value of the residual aberrations is close to $\lambda/40$. This deformable mirror has the potential to be used for astronomical adaptive optics.

Acknowledgments

This work is supported by the National Natural Science Foundation of China (Grant No. 11303019) and China Postdoctoral Science Foundation (No. 2013M531521), the Material Science and Technology Center Development Foundation of Hefei (No.2012FXCX002), Ningbo Natural Science Foundation (2013A610047), and Project of Education Department of Zhejiang Province (Y201326728).

Reference

- [1] M.A. Ealey, J.T. Trauger, SPIE, "High-density deformable mirrors to enable coronagraphic planet detection," *Proc. SPIE* **5166**, 172-179 (2004).
- [2] C.H. Rao, L. Zhu, X.J. Rao, C.L. Guan, D.H. Chen, S.Q. Chen, J. Lin, Z.Z. Liu, "Performance of the 37-element solar adaptive optics for the 26cm solar fine structure telescope at Yunnan Astronomical Observatory," *Appl. Opt.* **49**(31), G129-G135 (2010).
- [3] Vdovin, G., Loktev, M., and Simonov, A., "Low-cost deformable mirrors: technologies and goals," *Proc. SPIE* 5894, 58940B (2005).
- [4] E. Dalimier, C. Dainty, "Comparative analysis of deformable mirrors for ocular adaptive optics," *Opt. Express* **13**, 4275-4285 (2005).
- [5] J.Q. Ma, Y. Liu, T. He, B.Q. Li, J.R. Chu, "Double Drive Modes Unimorph Deformable Mirror for Low-Cost Adaptive Optics," *Appl. Opt.* **50**(29), 5647-5654(2011).
- [6] Horsley, D. A., Park, H., Laut, S. P., and Werner, J. S., "Characterization of a bimorph deformable mirror using stroboscopic phase-shifting interferometry," *Sensors and Actuators a-Physical* **134**(1), 221-230 (2007).
- [7] Samarkin, V., and Kudryashov, A., "Deformable mirrors for laser beam shaping," *Proc. SPIE* 7789, 77890B (2010).
- [8] X. H. Xu, B. Q. Li, Y. Feng, and J. R. Chu, "Design, fabrication and characterization of a bulk-PZT-actuated MEMS deformable mirror," *J. Micromech. Microeng.* **17**, 2439-2446 (2007).
- [9] M. Q. Bu, T. Melvin, G. Ensell, J. S. Wilkinson, and A. G. R. Evans, "Design and theoretical evaluation of a novel microfluidic device to be used for PCR," *J. Micromech. Microeng.* **13**, 125-130 (2003).